Obliquely Truncated Simple Horns: Idealized Models for Vertebrate Pinnae

by N. H. Fletcher

Institute of Physical Sciences, CSIRO, Limestone Avenue, Canberra ACT 2602, Australia

and Suszanne Thwaites

Division of Applied Physics, CSIRO, Bradfield Road, Lindfield NSW 2070, Australia

Summary

The acoustical behaviour of simple horns of parabolic, conical and exponential profile is analyzed and explicit expressions are given for the impedance coefficients Z_{ij}. Wavefront curvature effects are included and the discussion is extended to investigate the effect of oblique truncation, which gives the horn a shape closely similar to that of a typical vertebrate pinna. The effects of higher modes are discussed qualitatively and the conditions under which these can be neglected are outlined. All horns are shown to act as efficient pressure transformers over only a restricted bandwidth, the limits of which are determined by flare rate and mouth diameter. For a horn with throat area S_1 and mouth area S_2 the maximum blocked-throat pressure gain is $10\log_{10}(4\,S_2/S_1)$ decibels; the gain reduces to 0 dB at low frequencies and may become negative at very high frequencies. Oblique truncation raises the maximum gain above that of a horn truncated normally with the same minimum throat-to-mouth distance. It also moves the axis of maximum acoustic response away from the geometric axis of the horn towards the normal to the oblique mouth. This shift is large at low frequencies, becomes slightly negative at mid frequencies, and approaches zero at high frequencies. Use of these results in the analysis of model auditory systems is outlined.

Schräg abgeschnittene, einfache Trichter: Idealisiertes Modell für die Pinnae von Wirbeltieren

Zusammenfassung

Es wird das akustische Verhalten von einfachen Trichtern mit parabolischem, konischem und Exponentialprofil untersucht, und es werden explizite Ausdrücke für die Impedanzkoeffizienten Z_{ij} angegeben. Dabei wird die Wirkung der Wellenfrontkrümmung eingeschlossen, und die Behandlung wird ausgedehnt auf die Untersuchung der Wirkung schrägen Abschneidens, was dem Trichter eine Form gibt, die der einer typischen Wirbeltier-Pinnae nahekommt. Die Effekte von höheren Wellenmoden werden qualitativ diskutiert und es werden die Bedingungen angegeben, unter denen sie vernachlässigt werden können. Es wird gezeigt, daß alle Trichter eine Drucktransformation nur über eine beschränkte Bandbreite bewirken, wobei die Bandgrenzen von der Öffnungsrate und dem Ausgangsdurchmesser bestimmt werden. Für einen Trichter mit dem Eingangsquerschnitt S_1 und dem Ausgangsquerschnitt S_2 ist der maximale Druckgewinn bei verschlossenem Eingang $10\lg(4\,S_2/S_1)$ Dezibel; der Gewinn verschwindet bei tiefen Frequenzen und kann bei sehr hohen Frequenzen negativ werden. Ein schräges Abschneiden erhöht den maximalen Gewinn über den eines gerade abgeschnittenen Trichters mit demselben Minimalabstand zwischen beiden Öffnungen. Es verschiebt außerdem die Achse maximaler akustischer Übertragung von der geometrischen Trichterachse auf die Normale der schrägen Ausgangsöffnung hin. Diese Verschiebung ist groß bei niederen Frequenzen, wird leicht negativ bei mittleren Frequenzen und verschwindet allmählich bei hohen Frequenzen. Es wird der Nutzen dieser Resultate bei der Analyse von Gehörmodellen dargelegt.

Les cornets simples à troncature oblique: des modèles idéaux pour les pavillons d'oreille des vertébrés

Sommaire

On rappelle le comportement acoustique des cornets aux profils les plus simples: parabolique, conique et exponentiel; on fournit aussi des expressions explicites pour leurs coefficients d'impédance Z_{ij}. On étend l'étude aux effets dus à la courbure des fronts d'onde dans le cornet. Puis on aborde l'étude des effets d'une troncature oblique, qui peut donner au cornet tronqué une forme approchant assez bien celle d'un pavillon d'oreille typique de vertébré. On examine qualitativement les effets des modes supérieurs en soulignant les conditions sous lesquelles ils peuvent être négligés. On observe que tous les cornets agissent bien comme des transformateurs de pression acoustique, mais seulement sur une bande de fréquences restreinte, dont les bornes sont déterminées par le diamètre de l'embouchure et le taux d'évasement du cornet. Pour un cornet dont la section droite est S_1 à la gorge et S_2 à l'embouchure, le gain maximal de pression (à entrée bloquée) est de $10\log_{10}(4\,S_2/S_1)$ dB; mais ce gain tombe à zéro dB aux basses fréquences et peut devenir négatif aux très hautes fréquences. Une troncature oblique élève le gain maximal au-dessus de celui d'un cornet semblable mais à

troncature normale, pourvu que soit respectée la distance gorge-embouchure. Elle décale aussi l'axe de la réponse acoustique maximale en l'écartant de l'axe géométrique du cornet pour le rapprocher de la normale à la troncature oblique. Ce décalage est important aux basses fréquences, puis il diminue pour devenir faible et négatif aux fréquences moyennes et retourne à zéro aux fréquences hautes. On insiste pour finir sur les applications de ces résultats pour analyser les modèles de systèmes auditifs.

Introduction

It is common knowledge that the external pinnae of animals such as cats, dogs and bats behave as acoustic horns to amplify the incident sound pressure and confer additional directional discrimination upon the auditory system. It is also generally well known that simple horns exhibit some sort of cut-off frequency above which they are efficient but below which their performance deteriorates. It is much less widely known that there is an upper cut-off frequency for horns of finite length above which their efficiency as acoustic receivers also falls to a low value.

Unfortunately the standard texts such as Morse [1], Beranek [2] and Olson [3] discuss horns only in a rather different context, and the same is true of the more specialist literature [4, 5]. Even publications dealing with auditory systems either deal with very limited aspects of the problem or else give insufficient detail about the general case [6].

Our purpose in the present paper, therefore, is to present an extended treatment of the behaviour of simple finite horns, particularly when the mouth opening is oblique to the horn axis, in such a form as to be useful in the analysis and understanding of auditory systems. The results are, however, of more general interest in acoustics, since they do not seem to have been given explicitly before.

We recognise from the outset that while an obliquely truncated horn of approximately conical profile is a good model for the pinna of an animal like the kangaroo, the cat and perhaps the bat, the same cannot be said of the pinnae of primates such as man. While there are traces of horn-like behaviour in such primate ears, the anatomy of the pinna is sufficiently convoluted and asymmetrical that its acoustical behaviour is better analyzed by using an entirely different idealized model [7, 8].

1. Response of a normally truncated horn

In most first-order treatments of acoustical systems it is adequate to use a one-dimensional formalism. For a horn this implies the neglect of duct modes other than those corresponding to plane-wave propagation, or perhaps spherical-wave propagation, in the horn, so that conditions at the mouth or throat are adequately specified by given the acoustic pressure p and volume flow U into the horn. Higher modes can in fact propagate from the mouth into the horn until the horn diameter becomes comparable with the sound wavelength, beyond which point such modes are attenuated. We will see later that such higher modes begin to have an effect at very high frequencies, even for symmetrical horns with symmetrically located pressure transducers. When symmetry is absent, higher modes may become important at lower frequencies [7]. It is, however, a good first approximation to consider only the lowest-order mode and initially to assume exact axial symmetry. We stress that here we are investigating the model system – real auditory systems will not satisfy our assumptions exactly [9].

If we adopt the definitions and sign conventions given in Fig. 1, then the acoustic behaviour of the horn is completely specified by the acoustic impedance coefficients Z_{ij} defined by

$$p_1 = Z_{11} U_1 + Z_{12} U_2, \tag{1}$$

$$p_2 = Z_{21} U_1 + Z_{22} U_2, \tag{2}$$

where $Z_{21} = Z_{12}$ and we assume a time variation $\exp(j\omega t)$. Solutions of the equation for wave propagation in a horn generally give the input impedance p_1/U_1 at the throat when the mouth is loaded with an external impedance Z_L [3, 10]. It is a matter of simple algebra to derive the coefficients Z_{ij} from these results. In the sections below we give explicit results for parabolic, conical and exponential horns, not because these are necessarily particularly good approximations to real auditory system components, but rather because they are analytically simple and comprise, between them, horn profiles with decreasing, constant, and increasing flare rates, as shown in Fig. 2. Indeed we shall find that, for typical rather short auditory horns, the acoustic behaviour is not very sensitive to

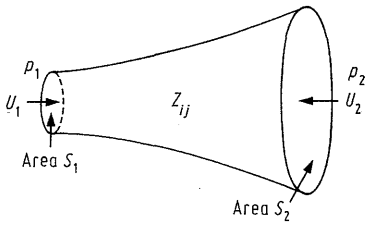

Fig. 1. Definition of acoustic quantities for a horn.

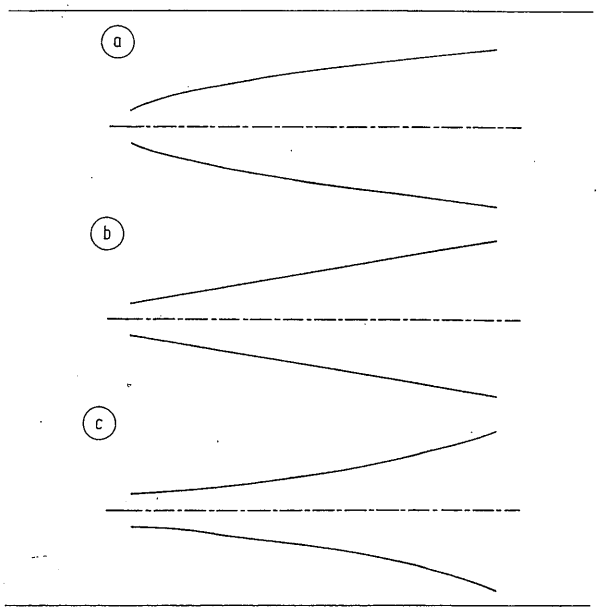

Fig. 2. Horn profiles: a) parabolic, b) conical, and c) exponential.

the horn profile, for a reasonable range of variation, once mouth and throat diameters and horn length have been specified.

1.1. Parabolic horn

The parabolic horn belongs to the family of Bessel horns [5] for which the cross-sectional area $S(x)$ at position x along the horn axis has the form

$$S(x) = S_0 x^m, \tag{3}$$

where m is a constant. For the parabolic horn $m = 1$. In this and other cases, $S(x)$ should strictly be the area of an appropriately curved wavefront, but it is usually adequate to set it equal to the normal horn cross-section.

If the throat and mouth areas are S_1 and S_2 respectively and the horn length l, then we can assign coordinates x_1, x_2 to the throat and mouth by

$$x_1 = l S_1/(S_2 - S_1), \quad x_2 = l S_2/S_2 - S_1). \tag{4}$$

The impedance coefficients are then found to be

$$Z_{11} = \frac{\mathrm{j}\varrho c}{S_1}\left[\frac{J_0(kx_1)N_1(kx_2) - J_1(kx_2)N_0(kx_1)}{J_1(kx_1)N_1(kx_2) - J_1(kx_2)N_1(kx_1)}\right], \tag{5}$$

$$Z_{22} = -\frac{\mathrm{j}\varrho c}{S_2}\left[\frac{J_0(kx_2)N_1(kx_1) - J_1(kx_1)N_0(kx_2)}{J_1(kx_2)N_1(kx_1) - J_1(kx_1)N_1(kx_2)}\right], \tag{6}$$

$$Z_{12} = -\frac{\mathrm{j}\varrho c}{(S_1 S_2)^{1/2}}\left[\frac{2}{\pi k(x_1 x_2)^{1/2}}\right] \cdot \left[\frac{1}{J_1(kx_1)N_1(kx_2) - J_1(kx_2)N_1(kx_1)}\right], \tag{7}$$

where ϱ is the density and c the speed of sound in air, $k = \omega/c$ where ω is the angular frequency, and J_n, N_n are respectively Bessel functions and Neumann functions (Bessel functions of the second kind) of order n.

1.2. Conical horn

For a conical horn we have $m = 2$ in eq. (3) above, and we can assign coordinates x_1 and x_2 to the throat and mouth respectively by the relations

$$x_1 = l S_1^{1/2}/(S_2^{1/2} - S_1^{1/2}), \quad x_2 = l S_2^{1/2}/(S_2^{1/2} - S_1^{1/2}). \tag{8}$$

If we write

$$k\theta_1 = \tan^{-1} k x_1, \quad k\theta_2 = \tan^{-1} k x_2 \tag{9}$$

then we find

$$Z_{11} = \frac{\mathrm{j}\varrho c}{S_1}\left[\frac{\sin k(l-\theta_2)\sin k\theta_1}{\sin k(l+\theta_1-\theta_2)}\right] \tag{10}$$

$$Z_{22} = -\frac{\mathrm{j}\varrho c}{S_1}\left[\frac{\sin k(l+\theta_1)\sin k\theta_2}{\sin k(l+\theta_1-\theta_2)}\right] \tag{11}$$

$$Z_{12} = -\frac{\mathrm{j}\varrho c}{(S_1 S_2)^{1/2}}\left[\frac{\sin k\theta_1 \sin k\theta_2}{\sin k(l+\theta_1-\theta_2)}\right]. \tag{12}$$

1.3. Exponential horn

For an exponential horn we can write

$$S(x) = S_0 \mathrm{e}^{2mx}, \tag{13}$$

where

$$m = (1/2l)\ln(S_2/S_1). \tag{14}$$

If we define the quantities b and b' by

$$b = \mathrm{j}b' = (k^2 - m^2)^{1/2} \tag{15}$$

then b is real above a cut-off frequency given by $k = m$ while b' is real below this frequency. If we further define

$$\theta = \tan^{-1}(m/b), \quad \theta' = -\mathrm{j}\tanh^{-1}(m/b') \tag{16}$$

then, for $k > m$ or $\omega > mc$,

$$Z_{11} = -\frac{\mathrm{j}\varrho c}{S_1}\left[\frac{\cos(bl+\theta)}{\sin bl}\right] \tag{17}$$

$$Z_{22} = -\frac{\mathrm{j}\varrho c}{S_2}\left[\frac{\cos(bl-\theta)}{\sin bl}\right] \tag{18}$$

$$Z_{12} = -\frac{\mathrm{j}\varrho c}{(S_1 S_2)^{1/2}}\left[\frac{\cos\theta}{\sin bl}\right] \tag{19}$$

while, for $k < m$ or $\omega < mc$

$$Z_{11} = -\frac{\varrho c}{S_1}\left[\frac{\cosh(b'l+\theta')}{\sinh b'l}\right] \tag{20}$$

$$Z_{22} = -\frac{\varrho c}{S_2}\left[\frac{\cosh(b' l - \theta')}{\sinh b' l}\right] \tag{21}$$

$$Z_{12} = -\frac{\varrho c}{(S_1 S_2)^{1/2}}\left[\frac{\cosh \theta'}{\sinh b' l}\right]. \tag{22}$$

1.4. Radiation impedance

In all the applications we shall be considering, the horn will have its mouth open to act as a sound receiver. We shall presently invoke the principle of reciprocity to examine this case, but first we need to know the radiation impedance for outgoing waves at the open mouth. The exact expression for a horn has not been evaluated and even that for an unbaffled cylindrical pipe is extremely complicated [11]. For our present purposes it will be adequate to use the approximations

$$Re(Z_R) \approx \begin{cases} 0.25\,(k a)^2\,(\varrho c/\pi a^2) & k a < 2 \\ (\varrho c/\pi a^2) & k a > 2 \end{cases} \tag{23}$$

$$\mathrm{Im}(Z_R) = \begin{cases} (0.6\,k a)\,(\varrho c/\pi a^2) & k a < 1.6 \\ (1.5/k a)\,(\varrho c/\pi a^2) & k a > 1.6 \end{cases} \tag{24}$$

where a is the radius of the horn mouth [12]. The errors involved in these approximations because of neglect of wavefront curvature do not significantly affect our results.

1.5. Wall losses

It is possible to include the effects of viscous and thermal losses to the walls by replacing k in the coefficients Z_{ij} by the complex quantity

$$k \to \omega/c + \mathrm{j}\,\bar{\alpha}, \tag{25}$$

where $\bar{\alpha}$ is an appropriate average of the attenuation coefficient for a section of circular pipe taken over the length of the horn. Since this attenuation coefficient is inversely proportional to the local horn radius a, we can write [13]

$$\bar{\alpha} \approx 10^{-5}\,\omega^{1/2}\,(1/a)_{\mathrm{Av}}, \tag{26}$$

where $\bar{\alpha}$ and $(1/a)$ are both in (metres)$^{-1}$ and the average of $(1/a)$ is taken over the whole horn length. In biological horns $\bar{\alpha}$ may be larger than suggested by (26) because of the presence of many fine hairs on the inner surface of the horn.

Inclusion of wall losses in this way complicates the formulae for the Z_{ij} and, since α does not scale directly with ka as do the other quantities, the immediate generality of some of the results is lost. It is simple to see, however, that insertion of (25) into the expressions for the Z_{ij} degrades quantities such as the blocked-throat gain, which we discuss in the next section, by a factor $\exp(-\bar{\alpha} l)$. For the pinnae of typical vertebrates this performance degradation is less than 1 dB, unless there is substantial loss contributed by hair inside the ear.

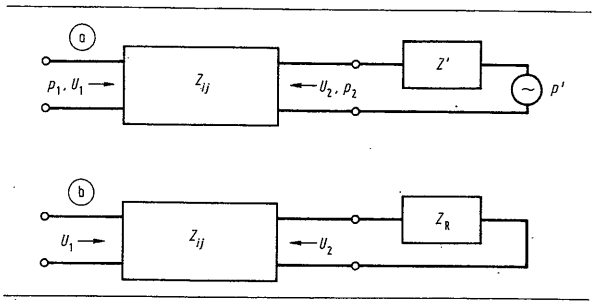

Fig. 3. a) Thévenin network for a horn excited by an axially incident plane wave. In this case $U_1 = 0$. b) Network for a driven horn radiating freely. Here $U_1 \neq 0$.

For horns of rather small flare rate, however, the damping of the lowest resonances may be provided largely by wall losses rather than by radiation from the mouth. Neglect of wall losses will therefore lead to unduly prominent peaks for these resonances. In what follows here, however, we omit any correction for wall losses in the interests of simplicity and generality. The moderately large flare rate of typical pinnae makes this reasonable.

1.6. The horn as a receiver

To evaluate the behaviour of a horn as an acoustic element receiving plane waves incident along its axis we expect to be able to treat the system as shown in Fig. 3 a. The incident plane wave with free-field pressure p_0 is represented, using Thévenin's theorem, by a pressure source of magnitude p' in series with an acoustic impedance Z', and we require to determine the values of these two quantities.

To do this we invoke the reciprocity theorem and calculate the pressure amplitude on the axis at a large distance R produced by a source of volume flow U_1 located in the otherwise blocked throat of the horn. This situation is shown in Fig. 3 b from which, using (2), we find

$$U_2 = -U_1\,Z_{21}/(Z_{22} + Z_R). \tag{27}$$

Treating the flow $-U_2$ as approximately equivalent to the same flow out of the end of an unbaffled pipe, we can evaluate the pressure $p(R)$ at R in the limits $ka \ll 1$ and $ka \gg 1$. If $ka \ll 1$ then the resistive part of the radiation impedance is only half that for a pipe set in an infinite baffle [14], so that the radiated power is less by 3 dB than in the baffled case. The radiation, moreover, is isotropic into a 4π solid angle rather than 2π as for the baffled case, so the radiated intensity on the axis is less by 6 dB. If $ka \gg 1$ however, the

radiation resistance is the same in each case and, except for minor side lobes, the angular distribution of intensity is nearly the same [15]. We therefore see that

$$p(R) = \begin{cases} -\mathrm{j}\varrho\omega U_2 \mathrm{e}^{-\mathrm{j}kR}/4\pi R & \text{for} \quad ka \ll 1 \\ -\mathrm{j}\varrho\omega U_2 \mathrm{e}^{-\mathrm{j}kR}/2\pi R & \text{for} \quad ka \gg 1 \end{cases}. \tag{28}$$

The transition between these two forms has no simple analytical representation, but it will be adequate for our present purposes to use the interpolation approximation

$$p(R) \approx -[\mathrm{j}\varrho\omega U_2 \mathrm{e}^{-\mathrm{j}kR}/4\pi R](1 + \tanh ka), \tag{29}$$

where U_2 is given in terms of U_1 by (27). There is no significance in the choice of a hyperbolic tangent function except that it gives a cross-over between the two forms of (28) of about the correct width at about the correct ka value.

Now, invoking the reciprocity theorem, a simple source of strength U_1 at R will produce a pressure $p(R)$, given by (29), in the blocked throat of the horn. But this simple source produces a free-field pressure

$$p_0 = \mathrm{j}\varrho\omega U_1 \mathrm{e}^{-\mathrm{j}kR}/4\pi R \tag{30}$$

at the mouth of the horn, so that from (27) and (29) we can write

$$\begin{aligned} p(R) &\approx -p_0(U_2/U_1)(1 + \tanh ka) \\ &\approx p_0(1 + \tanh ka) Z_{21}/(Z_{22} + Z_R). \end{aligned} \tag{31}$$

Comparison of this result with that for p_1 in the network of Fig. 3a shows that the incident plane wave behaves like a pressure generator with

$$p' \approx p_0(1 + \tanh ka), \quad Z' = Z_R. \tag{32}$$

The effective source pressure p' thus doubles from the free-field to the infinite-baffle value as ka goes from small to large relative to unity.

1.7. *Wavefront curvature*

At high frequencies the effect of mismatch between the curved wavefront in the horn and the plane wave incident from along the axis becomes significant. If we consider only the lowest transverse mode then, to a good approximation, the wavefront in the horn is a spherical cap with radius of curvature determined by the local flare angle of the horn as shown in Fig. 4. This is true at low frequencies for all horn shapes with moderately small flare [5] and is also clearly true for a conical horn in the high-frequency "optical" limit. Higher modes upset this generalization at high frequencies for horns with nonuniform flare, but these modes can be neglected to a first approximation in our present application, as we discuss later. If α is the semi-angle of the cone locally tangent to the horn at its mouth as shown, then the phase mismatch at a

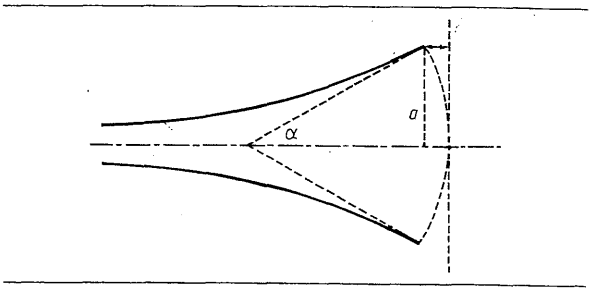

Fig. 4. Wavefront curvature at the mouth of a horn.

distance r from the axis is

$$\phi(r) \approx ka(r/a)^2 \tan\alpha/2 \tag{33}$$

and the effective pressure coupling the incident plane wave to spherical wave is no longer p' but rather

$$p'' = \frac{1}{\pi a^2} \int_0^a p' \mathrm{e}^{-\mathrm{j}\phi(r)} 2\pi r \,\mathrm{d}r \tag{34}$$

or, neglecting phase,

$$F_\alpha(ka) = |p''/p'| = \sin(\tfrac{1}{2}ka\tan\alpha/2)/(\tfrac{1}{2}ka\tan\alpha/2). \tag{35}$$

If, instead of having an incident plane wave, we have an incident spherical wave from a source at distance R along the axis, then we should make the replacement

$$\tan\alpha/2 \rightarrow \tan\alpha/2 + a/2R \tag{36}$$

in (35).

The effect of the correction (35) from p' to p'' is negligible at low frequencies but it reduces the horn response at high frequencies. The effective driving pressure p'' becomes zero when

$$ka = \frac{2n\pi}{\tan\alpha/2} \tag{37}$$

or as modified by (36).

To be completely consistent, we should really have included the effects of wavefront curvature in the discussion leading up to (32). To do this we introduce a correction factor which is simply $F_\alpha(ka)$ into (28) and (29), and it reappears in (32) in exactly the manner discussed above.

1.8. *Higher modes*

At frequencies high enough that wavefront curvature produces a significant effect, an incident plane wave will also excite higher modes within the horn. These modes will propagate towards the throat of the horn until the sound wavelength becomes nearly equal to the local horn diameter. Beyond this cut-off point the mode in question will have infinite phase velocity and large attenuation.

If the pressure transducer in the throat of the horn responds only to the lowest horn mode, then the presence of higher modes has no effect. A plane-piston coupling meets this condition. For other transducer couplings such as a flexible diaphragm, however, the response to the second axisymmetric mode may not be much less than that to the first mode [16]. For a flexible diaphragm stretching right across the horn throat, response to the second axisymmetric mode can be shown by simple integration to be about – 12 dB relative to response to the first mode. Higher modes that are not axisymmetric will, however, have no effect provided that the transducer is axisymmetric. The interaction of two or more modes will clearly depend on details of the transducer and horn-throat geometry, but we may expect it to shift the positions of the response zeros given by (37). In general, however, the envelope of $F_\alpha(k\,a)$ should provide an approximate upper limit to the envelope of the actual response. The exact treatment of these higher modes will be the subject of another publication.

1.9. Horns in acoustic systems

The acoustic behaviour of a horn as a receiver of axially incident sound is specified by the network of Fig. 3 a, with the definitions (32) and (35) determining the driving pressure. In principle any acoustic system can be coupled to the throat of the horn – typically a short cylindrical meatus, a heavily damped resonant tympanum and a backing cavity – and standard methods can then be used to analyse the whole system [6].

It is not our purpose to do this here, but it is appropriate to present the results of a few calculations and measurements to illustrate the general behaviour. To do this we have selected the case of a horn the throat of which is blocked by a measuring microphone of high acoustic impedance. Such a system presents no disposable parameters and is easily reproduced. It bears only a small relation to auditory systems, in which the impedance of the tympanum is usually only two or three times the input impedance at the horn throat.

The acoustic gain p_1/p_0 of such a system relative to the free field is readily calculated and, in decibel terms, has the value

$$G(k\,a) = 20\log_{10}\left\{\left[\frac{Z_{12}}{Z_{22}+Z_R}\right](1+\tanh k\,a)\,F_\alpha(k\,a)\right\}, \tag{38}$$

where $F_\alpha(k\,a)$ is given by (35). G cannot be written as a function of $k\,a$ alone if wall losses are included, as we remarked before.

Reference to the explicit forms for the Z_{ij} given in (5) to (22) and the limiting forms of Z_R given in (23) to (24) allows us to remark that in the horns considered, and indeed for any reasonably smooth horn profiles,

$$\lim_{ka\to 0} G(k\,a) = 0\,\text{dB} \tag{39}$$

while in the range $k\,a \gg 1$ but before the fall in $F_\alpha(k\,a)$

$$G(k\,a) \to 10\log_{10}(4\,S_2/S_1). \tag{40}$$

For higher frequencies still, $F_\alpha(k\,a) \ll 1$ and $G(k\,a) < 0$.

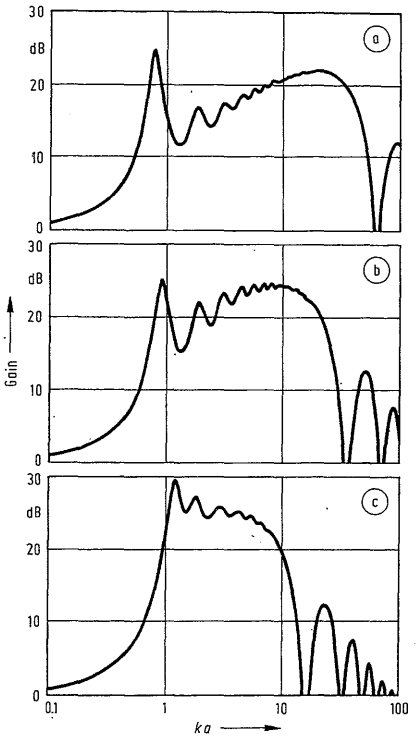

Fig. 5. Calculated curves for the gain of horns of (a) parabolic, (b) conical, and (c) exponential profile for an axially incident plane wave when the measuring microphone blocks the horn throat and responds only to the lowest mode. The mouth radius is a, the throat radius 0.1 a and the length 2.5 a in each case, and $k\,a$ is a frequency parameter ($k = \omega/c$).

Three typical examples for parabolic, conical and exponential horns with the same mouth and throat diameters and the same length are shown calculated in Fig. 5. Calculations took only a few minutes on a small desk-top computer. Clearly the horn is an efficient acoustic transformer over only a limited frequency band. There is a significant but not very large difference between the response curves for the three horns calculated.

Fig. 6 compares the measured response for a conical horn of axial length 192 mm, mouth diameter 148 mm and throat diameter 7 mm excited by an axial source at a distance of 1.7 m with the calculated response. The horn was constructed of 16 gauge aluminium in such a way that a 1/4 inch condenser microphone fitted snugly in the throat. The microphone

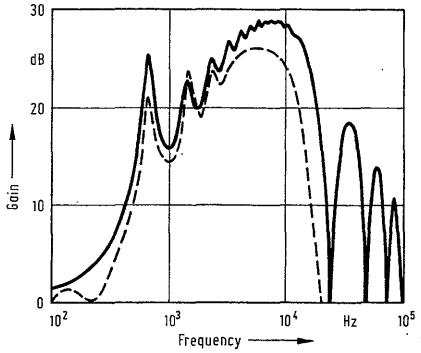

Fig. 6. Calculated gain curve for a conical horn of semi-angle 20°, mouth diameter 148 mm and throat diameter 7 mm with the microphone blocking the horn throat and responding only to the lowest mode. The broken curve shows the measured response with a normal condenser microphone.

output was recorded as a function of frequency from 100 Hz to 30 kHz and from this was subtracted the corresponding curve for the same microphone located in the free field at the position of the horn mouth (in the absence of the horn) to give the horn response. The agreement is acceptable over the whole frequency range.

The differences between the two curves can be accounted for, qualitatively, from known shortcomings in both theory and experiment. In the first place the calculations neglect wall losses as described by (25) and (26). Inclusion of these losses woul lower the calculated gain curve, particularly at high frequencies, but the extent of this lowering is less than 1 dB at 10 kHz. Similarly the allowance for the finite acoustic impedance of the microphone would further lower the curve, but this effect is again considerably less than 1 dB.

The residual disagreement at low frequencies can be ascribed in part to inadequacies in the interpolation formula (29) and in part to the effects of wall reflections in the experiment. The residual disagreement at high frequencies is almost certainly due to neglect of higher modes within the horn. The experimental curve lies below the theoretical curve and the first zero is shifted, which is what our discussion would lead us to expect. The experimental curve does have further maxima and minima above 20 kHz of about the magnitude expected, but their frequencies are not in good agreement with those predicted for the first mode alone.

2. Directionality of obliquely truncated horns

From a consideration of the complexity of a rigorous calculation of the radiation from a normally truncated cylindrical pipe [11] it is clear that no really accurate quasi-analytical calculation of the radiation pattern, or equivalently the angular response, of an obliquely truncated horn can be attempted. On the other hand the problem is physically interesting and its applicability as a model for vertebrate pinnae is sufficiently close that even a rather roughly approximate treatment may give valuable insight. It is in this spirit that we proceed. The methods are applicable to any sort of horn and any geometry of truncation, but for simplicity we limit discussion to conical horns.

Our method of approach relies upon integration of the primary radiation pattern produced by sources distributed over the normal mouth of the horn, upon which is superposed the radiation pattern produced by coherent scattering of this primary beam from the sloping upper wall of the cone. The accuracy of the calculation does not warrant inclusion of secondary scattering of this beam.

The heart of the difficulty is the lack of any appropriate point-source radiation function (Green function) for the complicated geometry of this problem. Indeed only the Green functions for the wave equation in the infinite region and in the semi-infinite region with a plane or conical boundary are readily available. We must therefore devise approximate Green functions applicable to the present problem.

2.1. *Approximate Green functions*

For simplicty we consider initially the velocity potential $d\psi$ produced at the point $\boldsymbol{r}$ by a source of strength dQ located at $\boldsymbol{r}'$. If we suppress the time variation factor $\exp(j\omega t)$, then in the infinite domain

$$d\psi = -\frac{dQ}{4\pi|\boldsymbol{r}-\boldsymbol{r}'|}e^{-jk|\boldsymbol{r}-\boldsymbol{r}'|} = dQ\,\mathcal{G}_0(\boldsymbol{r},\boldsymbol{r}'), \quad (41)$$

where $\mathcal{G}_0(\boldsymbol{r},\boldsymbol{r}')$ is the free-space Green function. Similarly, if we consider the velocity potential generated by the same source dQ lying this time on an infinite baffle, then its image in the baffle doubles its effective source strength (while restricting its radiation solid angle to 2π) and the appropriate Green function is

$$\mathcal{G}_\infty(\boldsymbol{r},\boldsymbol{r}') = -\frac{1}{2\pi|\boldsymbol{r}-\boldsymbol{r}'|}e^{-jk|\boldsymbol{r}-\boldsymbol{r}'|}. \quad (42)$$

Our first task is to devise a Green function $\mathcal{G}_a(\boldsymbol{r},\boldsymbol{r}')$ for a point source lying on a circular baffle of radius a. We know that, in the far-field where $|\boldsymbol{r}-\boldsymbol{r}'| \gg a$

$$\begin{aligned} \mathcal{G}_a^F(\boldsymbol{r},\boldsymbol{r}') &\to \mathcal{G}_0(\boldsymbol{r},\boldsymbol{r}') \quad \text{for} \quad ka \ll 1 \\ \mathcal{G}_a^F(\boldsymbol{r},\boldsymbol{r}') &\to \mathcal{G}_\infty(\boldsymbol{r},\boldsymbol{r}') \quad \text{for} \quad ka \gg 1. \end{aligned} \quad (43)$$

It is thus a reasonable approximation to take

$$\mathcal{G}_a^F(\boldsymbol{r},\boldsymbol{r}') \approx \mathcal{G}_0(\boldsymbol{r},\boldsymbol{r}')(1+\tanh ka). \quad (44)$$

Azimuthal variation around the axis of the disc has been neglected for simplicity because we will usually be integrating over this angular coordinate. No particular significance should be attached to the analytic form of the factor in (44), as in the related expression (29).

In the very near field, $r \ll a$. we clearly have, for all $k\,a$,

$$\mathcal{G}_a^{\mathrm{N}}(\boldsymbol{r},\boldsymbol{r}') \to \mathcal{G}_\infty(\boldsymbol{r},\boldsymbol{r}') = 2\,\mathcal{G}_0(\boldsymbol{r},\boldsymbol{r}'). \qquad (45)$$

In the near field, $r \sim a$, where most reflections occur, (45) gives approximately the correct strength for the field but is less accurate in relation to the direction of the gradient. An interpolation formula would necessarily be rather arbitrary and, in the interests of simplicity, we therefore use $2\,\mathcal{G}_0$ as a reasonable approximation in the near field.

The second Green function we require relates to scattering or reflection from the walls of the horn. The procedure is to calculate the velocity potential, and thence the velocity, at these walls and superpose a source distribution that will cancel the motion of the fluid at the position of the wall. To achieve this we require an appropriately phased doublet distribution over the wall, with sources on opposite sides being π out of phase.

Again we know limiting forms for the Green function for this case. If γ is the angle between $\boldsymbol{r}$ and the normal to the surface, then the far-field doublet Green function for a large baffle has the form

$$\mathcal{G}_a^{\pm}(\boldsymbol{r},\boldsymbol{r}') \approx 2\,\mathcal{G}_0(\boldsymbol{r},\boldsymbol{r}')\cos\gamma \quad \text{for} \quad k\,a \gg 1. \qquad (46)$$

Similarly for a very small baffle we have just a simple doublet and the far-field Green function is

$$\mathcal{G}_a^{\pm}(\boldsymbol{r},\boldsymbol{r}') \approx \mathcal{G}_0(\boldsymbol{r},\boldsymbol{r}')\,k\,a\cos\gamma \quad \text{for}\, k\,a \ll 1. \qquad (47)$$

If we neglect details of interference effects on the basis that these will average out, then an appropriate interpolation between these forms is

$$\mathcal{G}_a^{\pm}(\boldsymbol{r},\boldsymbol{r}') \approx \mathcal{G}_0(\boldsymbol{r},\boldsymbol{r}')\tanh k\,a\,(1+\tanh k\,a)\cos\gamma. \qquad (48)$$

In this case, since we are not concerned with secondary scattering, we do not need a near-field Green function.

It is reassuring to remark that the results of the final numerical calculation are not very sensitive to the exact forms assumed for these Green functions. Indeed, simple use of $2\,\mathcal{G}_0$ throughout gives qualitatively similar results.

2.2. *Calculation*

The formal calculation is straightforward, though rather complicated. The principles can be understood by reference to Fig. 7. The conical horn is assumed to have a semi-angle α and a truncation angle β as shown ($\beta = 90°$ for normal truncation). The "normal mouth" AOB has radius a.

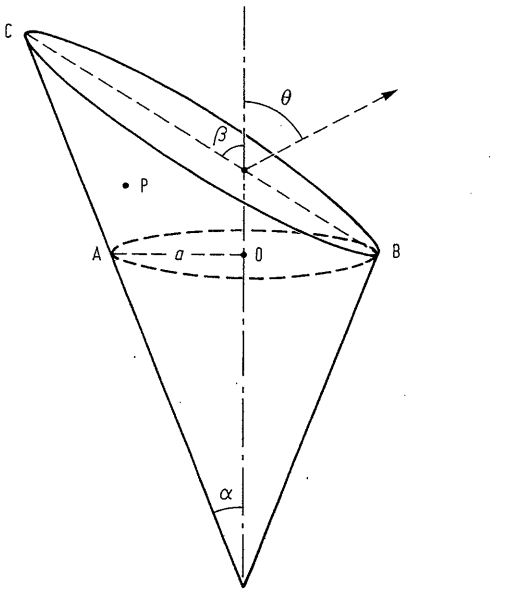

Fig. 7. A horn of semi-angle α, truncated obliquely at angle β. The normal mouth radius is a.

The calculation proceeds as a radiation problem, which is equivalent to the reception problem by reciprocity. The normal mouth AB is covered by sources of unit strength per unit area and the velocity potential ψ at each point P of the sloping wall is calculated using the near-field Green function $\mathcal{G}_a^{\mathrm{N}}$ given by (45). The acoustic velocity in the direction of the normal $\boldsymbol{n}$ to the reflecting surface at P is calculated as

$$v = -\,\boldsymbol{n}\cdot\nabla\psi \qquad (49)$$

and a doublet source density $\mp\,v$ per unit area is distributed on the surface at P, the sign of the source density on the inside wall being negative.

When this has been completed for all points P, the velocity potential radiated in direction θ to the cone axis is calculated, using $\mathcal{G}_a^{\mathrm{F}}$ given by (44) for the normal mouth and $\mathcal{G}_a^{\pm}$ given by (48) for the reflecting walls. In this latter Green function, a is really some average of the distance of each individual point P from the edge of the wall, and clearly the normal mouth radius is an adequate approximation to this. Finally, since pressure is directly proportional to velocity potential at any given frequency, the angular distribution of intensity is readily calculated. By appropriate normalization, the response at angle θ can be compared with the on-axis response for a normally truncated cone of mouth radius a.

2.3. *Results*

For a normally truncated cone the axis of maximum sensitivity corresponds, of course, to the geometric axis. By beginning with a constant acoustic flow in the horn mouth we confine ourselves to discussing a factor $H_\beta(ka, \theta)$ that would multiply the horn gain discussed in Section I of this paper, the axial response for a normally truncated horn being taken as the reference level.

Two particular horns were calculated in detail using the procedure set out above. Both had semi-angle $\alpha = 20°$ and the angles of truncation β were 30° and 60° respectively. The 30° horn was qualitatively very similar in shape to the pinna of a rabbit or kangaroo. The calculations required only a few minutes on a small desk-top computer.

In general for an obliquely truncated horn the axis of maximum sensitivity does not coincide with the geometric axis. For $ka < 1$ the response maximum is broad, as is to be expected, and is directed at a large positive angle θ^* to the axis. As ka increases, θ^* decreases sharply and may become negative for ka greater than about 2. The calculated behaviour for the two horns is shown in Figs. 8 and 9 respectively. The limiting behavior as $ka \to 0$ is not well defined in the calculations, since the primary lobe of the angular pattern becomes very broad for $ka < 1$, as indicated by the -3 dB curves in the figures, and the exact direction θ^* is sensitive to the precise form of the approximate expression (48). This is not important in a practical sense, since the response is nearly isotropic for $ka < 0.5$.

Also shown in these figures is the calculated gain $H(\theta^*)$ in the direction of maximum sensitivity relative to the on-axis gain of a normally truncated horn. $H(\theta^*)$ is 0 dB for $ka \ll 1$, goes through a broad maximum near $ka = 1$, and then declines slowly towards 0 dB as ka increases further. The maximum value of $H(\theta^*)$ is about + 6 dB for a horn truncated at 30° and + 3 dB for a horn truncated at 60°. Such an increase of gain is, of course, to be expected because of the increased mouth area.

To check the calculations, measurements were made on two metal horns in an anechoic chamber. These horns were also made out of aluminium and were truncated at angles, $\beta = 30°$ and 60°. The axial distance from the throat to the beginning of the mouth was 192 mm, the mouth diameter at this point was 148 mm and the throat diameter was 7 mm, all corresponding to the normally truncated horn measured earlier. The throat fitted into a face plate over a high power one inch dome tweeter.

With a microphone placed about 1.7 m from the throat, and the horn mounted on a turntable, polar

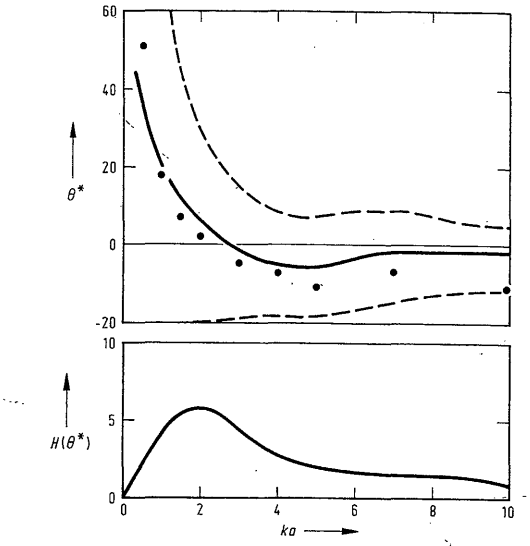

Fig. 8. Calculated angle θ^* of maximum response and gain $H(\theta^*)$ at that angle relative to the axial gain of a normally truncated horn, for a conical horn of semi-angle $\alpha = 20°$ truncated at an oblique angle $\beta = 30°$. Broken curves show the angles at which the response is 3 dB down from its maximum, and points are the results of measurements. The radius of the normal mouth of the horn is a, and ka is a frequency parameter ($k = \omega/c$).

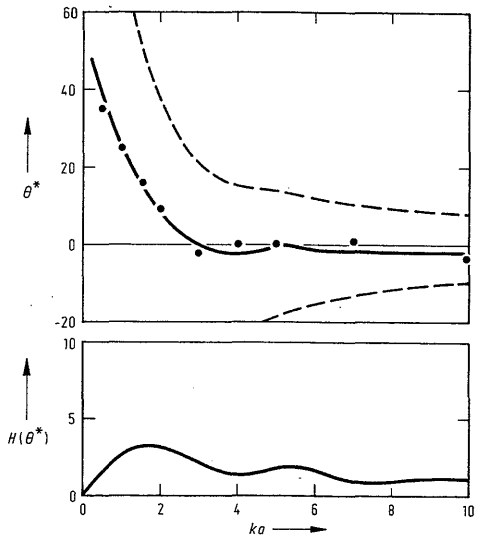

Fig. 9. As for Fig. 8 for a horn truncated less obliquely with $\beta = 60°$.

radiation patterns were obtained for ka values ranging from 0.5 to 10. The angle of maximum gain, θ^*, was read from these and is shown plotted as points in Figs. 8 and 9. The uncertainties involved in aligning the horn and the receiving microphone and in reading θ^* from the polar pattern amounted to about $\pm$ 5° for each point. There was some difficulty in achieving all the desired experimental conditions because of the range of ka values involved. The horn truncated at

$\beta = 30°$ was 0.9 m long. Consequently, the measurements were made at a rather modest distance and were not in the true far field. Nevertheless, they confirm the conclusions reached in the calculations.

It is clearly possible to perform similar calculations for horns with different profiles. The general nature of the analysis given above leads to the conclusion that such horns should show similar deflection of the direction of maximum sensitivity away from the horn axis at low frequencies and a similar increase in gain. Geometrical considerations suggest that the conical horn represents an intermediate case, with the directional shift θ^* being relatively smaller for an exponential and larger for a parabolic horn.

3. Discussion

The two parts of this paper can now be combined to give the total acoustic behaviour from an obliquely truncated horn. We have considered this explicitly only for the case of a conical horn but other profiles can be treated similarly. The conical horn is a close enough approximation to the pinnae of animals such as kangaroos, rabbits and bats to give a reasonable approximation to the behaviour to be expected.

In Part I we evaluated the parameters Z_{ij} and the source parameter p'' from which the behaviour of a normally truncated horn acting as an input coupler from the free field p_0 to the rest of an auditory system could be calculated.

As a particular case we calculated in (38) a universal expression for the simple case in which the auditory system was replaced by a pressure microphone of large acoustic impedance. This was expressed as an on-axis gain function $G(k\,a)$. For a horn truncated obliquely at an angle β less than 90°, we have calculated in Part II the gain $H_\beta(k\,a, \theta)$ at angle θ, relative to the gain of a normally truncated horn. This factor essentially multiplies the input pressure p''. If $H_\beta(k\,a, \theta)$ is expressed in decibels then it can be simply added to the on-axis gain $G(k\,a)$ given by (38). The calculation of $H_\beta(k\,a, \theta)$ gives the direction θ^* of maximum sensitivity for any value of $k\,a$ and also the effective beam width of the horn in the θ direction. For reference we note that the angular response of a normally truncated horn has approximately the form

$$H_{90}(k\,a, \theta) \approx 2\,J_1(k\,a \sin\theta)/k\,a \sin\theta \qquad (50)$$

where J_1 is a Bessel function of order 1 [17]. This expression actually applies only for single-mode propagation and with an infinite surrounding baffle. It is, however, a good approximation in the unbaffled case within the primary lobe region where $k\,a \sin\theta \lesssim 4$. From (50) the angular width of the response decreases with increasing frequency and this decrease is very similar in the case of oblique truncation, as shown by the 3 dB-down curves of Figs. 8 and 9.

Strictly one minor modification is required in this analysis because the radiation impedance Z_R of an obliquely truncated horn is somewhat larger than that of a normally truncated horn. The main effect is to shift the first horn resonance, clearly visible in Fig. 5, to a slightly lower frequency. This shift will, however, generally not exceed about 10 percent of the resonance frequency and so can be neglected.

When the horn is considered as a component of a more complex auditory system, as is usually the case, then we may wish to calculate the motion of a tympanum, or the pressure in front of it, for comparison with experiment. The way in which this can be done has been set out elsewhere [6]. The present analysis provides all the mechanism for doing this by giving the horn coefficients Z_{ij}, the cut-off function $F_\alpha(k\,a)$, the obliquity function $H_\beta(k\,a, \theta)$, and the total effective source pressure

$$p' \approx p_0(1 + \tanh k\,a)\,F_\alpha(k\,a)\,H_\beta(k\,a, \theta), \qquad (51)$$

where p_0 is the free-field pressure in a plane wave incident from direction θ. To avoid unduly emphasizing the lower resonances of the horn it will generally be necessary to include wall losses through eqs. (25) and (26) as well as in other parts of the system. It is not our intention here to give any detailed application of these results to auditory systems, though it is straightforward to extend results such as (38) to the case in which, rather than being blocked at the throat, the horn terminates in a damped resonant tympanum in front of which the pressure p_1 is measured. If the impedance of the tympanum is Z_T then we simply make the replacement

$$\frac{Z_{12}}{Z_{22} + Z_R} \to \frac{Z_{12}\,Z_T}{(Z_{22} + Z_R)(Z_{11} + Z_T) - Z_{12}^2} \qquad (52)$$

in (38). The two expressions are clearly equivalent in the limit $Z_T \to \infty$, while the gain is substantially reduced if $Z_T < Z_{11}$.

A similar, though more complicated, extension can be made to the case where the tympanum is connected to the horn throat by a short cylindrical meatus. The calculated behaviour of such a system for the case where Z_T is a few times Z_{11} exhibits a gain behaviour broadly similar to that of the blocked-throat horn and has the same direcitonal properties. Measurements made in this way on kangaroo ears [18] show horn gain, horn bandwidth, and shift of axis of greatest sensitivity in semi-quantitative agreement with the predictions of our model.

(Received July 28th, 1987.)

Note added in proof:

Attention should be drawn to the work of Dezso [19] who has calculated the axial radiation from a horn in an infinite baffle, including a correction for wavefront curvature. His results agree generally with ours for this case when allowance is made for the presence of the baffle.

References

[1] Morse, P. M., Vibration and sound. McGraw-Hill, New York 1948; reprinted American Institute of Physics, New York 1976, pp. 265–293.
[2] Beranek, L. L., Acoustics. McGraw-Hill, New York 1954; reprinted American Institute of Physics, New York 1986, pp. 259–284.
[3] Olson, H. F., Acoustical engineering. Van Nostrand, Princeton 1957, pp. 101–115.
[4] Eisner, E., Complete solutions of the "Webster" horn equation. J. Acoust. Soc. Amer. **41** [1967], 1126–1146.
[5] Benade, A. H. and Jansson, E. V., On plane and spherical waves in horns with nonuniform flare, I. Acustica **31** [1974], 80–98.
[6] Fletcher, N. H. and Thwaites, S., Physical models for the analysis of acoustical systems in biology. Quart. Rev. Biophys. **12** [1979], 25–65 and 463.
[7] Teranishi, R. and Shaw, E. A. G., External ear acoustic models with simple geometry. J. Acoust. Soc. Amer. **44** [1968], 257–263.
[8] Shaw, E. A. G., The external ear. In: Handbook of Sensory Physiology, ed. W. D. Keidel and W. D. Neff. Springer-Verlag, New York 1974, Vol V/1, pp. 455–490.
[9] Khanna, S. M. and Stinson, M. R., Specification of the acoustical input to the ear at high frequencies. J. Acoust. Soc. Amer. **77** [1985], 577–589.
[10] Morse, P. M., ref. [1] pp. 283–285.
[11] Levine, H. and Schwinger, J., On the radiation of sound from an unflanged circular pipe. Phys. Rev. **73** [1948], 383–406.
[12] Beranek, L. L., ref. [2] p. 122, Fig. 5.7.
[13] Benade, A. H., On the propagation of sound waves in a cylindrical conduit. J. Acoust. Soc. Amer. **44** [1968], 616–623.
[14] Beranek, L. L., ref. [2] p. 119, Fig. 5.3; p. 122, Fig. 5.7.
[15] Beranek, L. L., ref. [2] p. 102, Fig. 4.10; p. 104, Fig. 4.12.
[16] Morse, P. M., ref. [1] pp. 197–198.
[17] Morse, P. M., ref. [1] pp. 326–328.
[18] Coles, R. and Guppy, A., Personal communication, 1985.
[19] Dezso, G., On calculation of free-field sound pressure response of an arbitrary shaped horn. Proc. 12th International Congress on Acoustics, Toronto 1986, paper G4–7.